# Framework for Developing Digital Twin Prototypes

**Vilius Portapas**
University of Nottingham
University Park, Nottingham, NG7 2RD
UNITED KINGDOM

vilius.portapas@nottingham.ac.uk

**Yaseen Zaidi**
University of the West of England
Coldharbour Lane, Bristol, BS16 1QY
UNITED KINGDOM

yaseen.zaidi@uwe.ac.uk

## *ABSTRACT*

*This paper presents an agile co-simulation framework for developing digital twin prototypes of novel flying vehicles. The framework enables rapid assessment of flying vehicles' performance and flying dynamics in the early stages of their design cycle. The framework integrates MATLAB/Simulink environment for flight dynamics modelling with the AGI STK Aviator mission simulator into a loose computational loop. The combination of two packages enables aircraft assessment not only from the flight dynamics perspective, but also from the overall mission perspective under GPS coverage and radar tracking.*

*The advantage of such a virtual flight test and evaluation framework is the faster development of new flying vehicles, imposing mission constraints from the early stages of their design cycle. Testing a prototype model in complex mission scenarios in varying conditions allows early identification of design limitations, hence improving the aircraft design process and reducing further design costs.*

*The paper concludes with an example of a civil eVTOL flight simulation between the two UK cities of Bristol and Cardiff. Modelling of the aerodynamics of eVTOL is based on look-up tables of numerically generated data, while the mission analysis is based on a GPS and radar surveillance capability of the aircraft along the route.*

## 1.0 INTRODUCTION

Incremental use of digital twins (DTs) in aerospace engineering has been evidenced during the last decades. The digital models of real vehicles have helped solve numerous problems since the very first introduction of DTs in the aerospace domain by NASA during its Apollo programme. Soon after introducing the term “digital twin” in 2002 by Dr. Grieves, NASA acknowledged advances in computational power and identified digital twins as the TOP 3 technical challenge in the domain of modelling, simulation and information technology [1]. The recent rise of urban air mobility (UAM) concepts, of which electric vertical take-off and landing (eVTOL) aircraft are the most popular ones, and advances in computational power suggest the potential use of digital twin prototypes (DTPs) in the early stages of aircraft design. DTPs allow the prediction of "the behaviour of the designed product with components that vary between its high and low tolerances to ascertain that the as-designed product met the proposed requirements" [2], and are also favoured by OEMs such as Boeing [3]. If successful, for the very first time in the history of commercial aerospace engineering this would allow testing an overall aircraft handling qualities before actual test aircraft is even built. This would allow for a quicker and less expensive certification process, which is critically important to start-up companies designing

and manufacturing eVTOLs [4]. Moreover, this could also reduce design-to-prototype timescales for military aircraft.

It is widely accepted that the first eVTOLs, although designed to be autonomous vehicles, will be tested in piloted configuration [5-6] and/or controlled remotely during the operations afterwards [4]. This implies that a thorough analysis of flying/handling qualities (FQs/HQs) and flight performance of the new vehicles is of paramount importance to ensure flight safety. The majority of eVTOLs are designed to take off and land as a helicopter and fly as an aeroplane, with the intermediate stage between vertical and horizontal flights called transition. HQs are usually established as requirements for certification, e.g. EASA CS-25 for large transport aeroplanes and EASA CS-29 for large helicopters. However, HQs for civil aircraft are usually very brief and flexible. It is opposite to HQs requirements for military aircraft [7-8], which are more precisely defined and based on so-called Mission Task Elements (MTEs). MTEs enable the differentiation of mission elements into separate tasks, e.g. initial take-off, climb, transition, etc. Moreover, the military domain led the development of FQs/HQs specifications for vertical/short take-off and landing (V/STOL) aircraft [9-11]. The most famous are the V-22 Osprey (propeller-driven) and Harrier/F-35 (both jet driven). The US Federal Aviation Administration used these military specifications as support while certifying AgustaWestland AW609 tiltrotor VTOL aircraft. Civil aircraft certification authorities use different methods for eVTOL certification, i.e. FAA uses the so-called hybrid approach, where requirements are taken from currently existing regulations, while EASA issued special condition requirements specifically for small-category VTOL aircraft [12].

The discussion above leads to the conclusion that the current regulations for eVTOL certification are rather flexible. Hence, the research project [13] was initiated in 2020 to investigate the potential of using digital tools for the certification of new eVTOL designs. This paper proposes the modelling and simulation framework to test the (e)VTOL aircraft design using MTEs as means to define flying/handling qualities and flight performance characteristics. The paper defines the developed framework, the aircraft under investigation, the mission, and discusses the results and suggests further directions for the development of the framework.

## 2.0 MODELLING AND SIMULATION FRAMEWORK

The proposed framework integrates the MATLAB/Simulink environment for flight dynamics modelling with the AGI STK Aviator mission simulator. Currently, the framework forms a loosely coupled computational loop as it requires the manual transfer of data between the two software packages.

Figure 1 presents the structure of the framework and identifies the flow of data between the two software packages. MATLAB/Simulink provides aircraft states, i.e. attitude and position, to STK Aviator, which models an environment that an aircraft is operating within. Such a combination of MATLAB/Simulink and STK Aviator enables the assessment of an aircraft from both flight dynamics and overall mission perspectives. For example, a set of objectives for the mission assessment could be GPS coverage and radar tracking of an aircraft during the mission. This framework enables not only the assessment of an aircraft's suitability for an intended mission but also a timely rectification of design issues in advance of manufacturing an actual artefact.

The analysis presented later in this paper shows a design issue of an eVTOL under investigation. The original mass distribution resulted in a centre of gravity (CG) position behind the neutral point of the aircraft. This means that an airframe would be inherently unstable – an undesirable situation that should be avoided if possible.

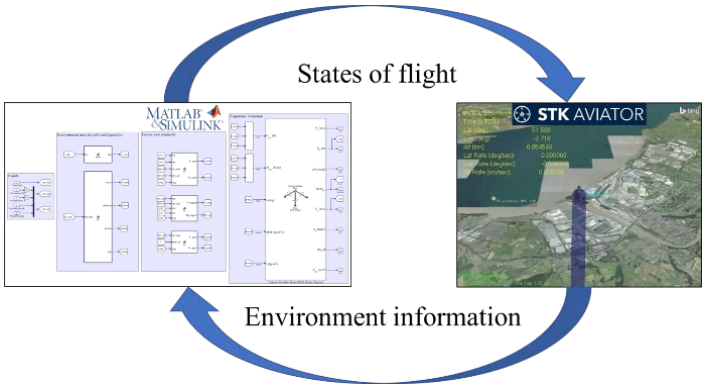


**Figure 1. Modelling and simulation framework architecture**

## 2.1 MATLAB/Simulink flight dynamics model

MATLAB/Simulink environment has been chosen for the framework to be developed as:

1) it allows quick changes to be made for a vehicle under investigation;

2) it allows the implementation of multiple vehicles and their parameters in an easy-to-use plug-and-play environment;

3) it is easy to learn for every engineer without requiring special knowledge of programming, hence it is broadly used across the aerospace engineering domain;

4) enables further developments of the framework within academia and industry.

This chapter reviews the current state of the framework and provides directions for its future development and parameters of an eVTOL used to verify the framework.

The current model has 3 degrees of freedom (3-DoF) to model the longitudinal flight. 6-DoF model will be implemented once the mechanics of the longitudinal eVTOL flight will be fully understood.

### 2.1.1 Forces and moments of wings

Aerodynamic forces and moments are calculated for the forward and rear wings, the cabin, and the frame.

The lift generated by the front and aft wings provides the main lifting capability during horizontal flight. Aerodynamic modelling of the wings is based on lookup tables for lift, drag and pitching moment coefficients ($C_L$, $C_D$ and $C_m$) that were calculated using JavaFoil v2.28, which uses the potential flow method and Prandtl's lifting line theory approximation for the finite wing [14]. The lift, drag and pitching moment of each wing is then expressed as:

$$L_w = \bar{q}C_L(Re,\alpha)\int_{-\frac{b}{2}}^{\frac{b}{2}} c(y)dy;\ D_w = \bar{q}C_D(Re,\alpha)\int_{-\frac{b}{2}}^{\frac{b}{2}} c(y)dy;\ M_w = \bar{q}\bar{c}C_m(Re,\alpha)\int_{-\frac{b}{2}}^{\frac{b}{2}} c(y)dy,$$

where $b$ is the semispan of a wing, $c(y)$ – chord length at spanwise position, $\bar{c}$ – mean aerodynamic chord of a wing, $\bar{q}$ – dynamic pressure, i.e. $\bar{q} = \frac{\rho V^2}{2}$ ($\rho$ – air density, $V$ – airspeed).

One of the biggest limitations of such an approach is that the flow is modelled as attached, hence no flow separation at high angles of attack. However, high angles of attack would most probably appear during the reconfiguration stage from the horizontal to vertical flight, when the frame with both wings would move by around 90° from horizontal to vertical position.

### 2.1.2 Forces and moments of control surfaces

Elevons are the only control surfaces distributed along the span of both wings with hinge location at 75% of the mean aerodynamic chord of the wings. They are currently modelled in a way that they deflect in the same direction on both sides of a wing, hence being used only for longitudinal flight control.

Figure 2 shows the positive and negative deflection of elevons in the case of the eVTOL configuration described later in this paper. The standard convention is used to determine the positive and negative deflection of elevons, i.e. positive elevon deflection creates a negative pitching moment around CG and negative elevon deflection creates a positive moment around CG. Application of this convention means that elevons are deflected in opposite directions for forward and rear wings as both wings are on the opposite sides of CG.

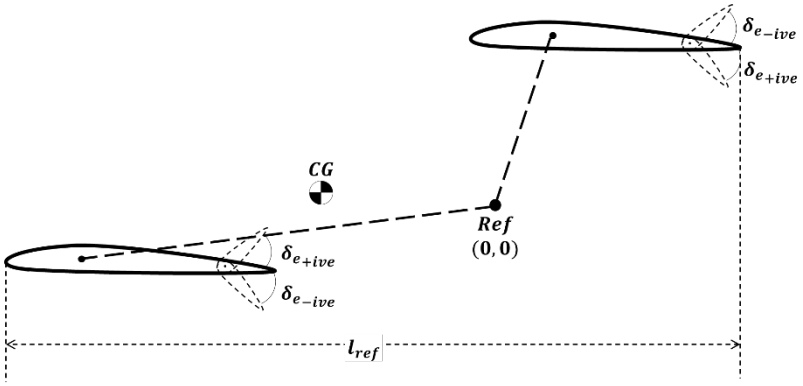


**Figure 2. Positive and negative elevon angles**

The contribution of each elevon to the overall aerodynamics of the wing is modelled as additional $\Delta C_{L_{\delta_e}}$, $\Delta C_{D_{\delta_e}}$ and $\Delta C_{m_{\delta_e}}$ contributions:

$$\Delta L_{w_{\delta_e}} = \bar{q}\Delta C_{L_{\delta_e}}(\alpha)\int_{-\frac{b}{2}}^{\frac{b}{2}} c(y)dy;\ \Delta D_{w_{\delta_e}} = \bar{q}\Delta C_{D_{\delta_e}}(\alpha)\int_{-\frac{b}{2}}^{\frac{b}{2}} c(y)dy;\ \Delta M_{w_{\delta_e}} = \bar{q}\bar{c}\Delta C_{m_{\delta_e}}(\alpha)\int_{-\frac{b}{2}}^{\frac{b}{2}} c(y)dy.$$

### 2.1.3 Other forces and moments

Thrust ($T$), power ($P$) and torque ($Q$) are calculated as functions of: $T = f(C_T, \rho, n, D)$, $P = f(C_P, \rho, n, D)$, $Q = f(C_Q, \rho, n, D)$, where $C_{T,P,Q}$ are coefficients of thrust, power and torque, $\rho$ – density of air, $n$ – revolutions per second of the propeller, $D$ – propeller diameter. However, $T$, $P$ and $Q$ are variables dependent on the advance ratio $J = \frac{V}{nD}$, where $V$ is the freestream velocity of air. For the example presented in this paper, relations *T(J)*, *P(J)* and *Q(J)* were provided by the designer of eVTOL under investigation.

Gravity forces are modelled as per the WGS-84 system [15]. The reference point for moment calculations is CG, hence there are no moments due to the gravity force.

## 2.2 STK Aviator flight environment model

Systems Tool Kit (STK) is a multi-domain digital mission engineering and systems of systems environment. It allows model integration of space, air, land, and sea infrastructure and related assets in realistic operating scenarios such as terrain imagery, radio wave propagation, interference, weather, and atmospheric conditions. Both physics and system-level fidelity models may be simulated.

STK Aviator allows analysis of the flight concept of operation and performance in 4-D trajectory in a single digital workspace comprising measurement data, multiple frames of reference and complex interaction of supported payload and platform systems such as observation instruments, flight controllers, fuel and power consumption, sensors, GPS, communication avionics, radar, and antenna coverage. The simulation is agile and renders quick evaluations of system behaviours through internal or external propagators. As such STK Aviator complements the previously discussed MATLAB/Simulink-based flight dynamics model with features that otherwise would be challenging to model and visualise within MATLAB/Simulink environment.

Primary surveillance radar coverage and GPS coverage were chosen as examples of the capabilities of the developed framework.

### 2.2.1 Primary surveillance radar coverage

The primary surveillance radar (PSR) was chosen as one of the examples to verify the framework. PSR's maximum line of sight slant range $R$ on the spherical Earth limited by the horizon could be estimated from the following relationship [16]:

$$R = 1.2\sqrt{h_T} + 1.2\sqrt{h_R},$$

where $h_T$ is the tower height and $h_R$ is the altitude of an aircraft, both in feet.

The ideal radar range equation shown below maximises the probability of detection through the transmit and receive power $P_t$ and $P_r$, signal wavelength $\lambda$, antenna gain $G$ and effective area $\sigma$ of the target that echoes the radiated power:

$$R^4 = \frac{P_t G^2 \lambda^2 \sigma}{(4\pi)^2 P_r}$$

Typically, the target height is not the issue for the primary surveillance radar as no aircraft would fly above 60,000 ft, but the targets are to be detected as far as 200 NM. This requirement stipulates a surveillance area for the target location as a very flat cylinder whose radius is significantly larger than its height [17]. Therefore, the radiated power pattern of the antenna is designed to spread in such an area to maximise the detection.

To spread the power over a flat cylinder, the equation may be written in terms of azimuth $\theta$ and elevation $\phi$ angles with the gain at the boresight $G$:

$$R^4(\theta, \phi) = k\, G^2(\theta, \phi)$$

The gain can be maximised with a shaping factor $f$ defined as the maximum diagonal range from the radar to the farthest edge of the beam pattern:

$$G(\theta, \phi) = G_{max}\, f(\theta, \phi)$$

The aircraft altitude $h$ and the elevation angle $\phi$ relate to the diagonal range $f$

$$\csc\phi = \frac{1}{\sin\phi} = \frac{f}{h}$$

Therefore,

$$G(\phi) = G_{max}\csc^2\phi$$

This cosecant squared beam shaping was key to correctly modelling the detection.

### 2.2.2 GPS coverage and position accuracy

GPS constellation of 31 satellites is an essential navigational and attitude determination aid for urban air mobility, especially for low-flying uncrewed aerial vehicles and drones. On-board GPS receivers provide time, altitude, latitude, and longitude by computing the time difference of signals reaching a receiver from different satellites. However, the availability of the signal is not guaranteed and flying over a GPS-denied environment may be encountered en route. Typically, four satellites are needed for minimal link availability. Even though, when a good signal is available, civil infrastructure and tall buildings may cause reflections and ground equipment may cause interference or jamming, severely affecting the quality of service and therefore the safety of the vehicle. Hence, showing the capability of predicting the GPS coverage when modelling the flight is deemed a very important aspect.

## 3.0 AIRCRAFT AND MISSION UNDER ANALYSIS

### 3.1 Mission: ferry flight between Avonmouth, England and Cardiff, Wales

The mission for the current case is a ferry flight between Avonmouth, England and Cardiff, Wales as shown in Figure 3. This mission was chosen as suitable for showcasing the benefits of eVTOL flights with respect to ground transportation modes within the area for the research project described in Ref. [13]. The time for the start of the simulation was chosen to be 11:00 on the 20th of October, 2021.


**Figure 3. Ferry flight between Avonmouth, England and Cardiff, Wales**

### 3.2 Neoptera's eOpter

Neoptera's eOpter eVTOL aircraft was developed as a modular system, allowing detachment of the frame from the cabin. Such configuration enables a quicker turnaround time as there is no need to wait for the batteries within the cabin to be recharged. The peculiarity of this airframe is that its frame is moving together with the wings and motors mounted on the frame. The eOpter eVTOL aircraft is shown in Figure 4.

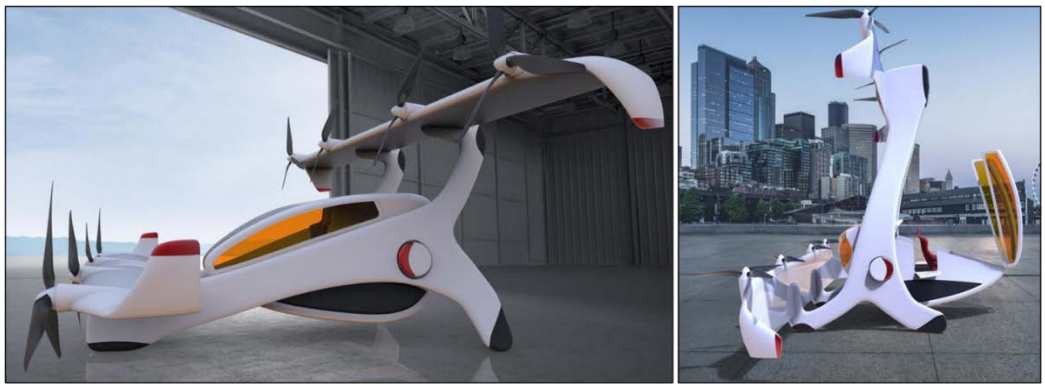

**Figure 4. Neoptera's eOpter in horizontal flight (left) and parking (right) configurations**

The eOpter has the dimensions presented in Table 1 and aerodynamic characteristics of the aerofoils as shown in Figure 5.

**Table 1. Main dimensions, mass and flight performance parameters of Neoptera's eOpter**

| **Dimensions of wings** | | **Mass** | |
|---|---|---|---|
| Wingspan, m | 6.44 | Airframe, kg | 854 |
| Area (front wing), $m^2$ | 4.23 | **Flight performance** | |
| Area (rear wing), $m^2$ | 5.52 | Cruise velocity, m/s | 55 |
| Elevon chord length | 25% of MAC | Endurance, min | 20 |
| $\bar{c}_{front}$, m | 0.66 | Range, km | 66 |
| $\bar{c}_{rear}$, m | 0.86 | **Other data** | |
| | | Propeller diameter, m | 1.65 |

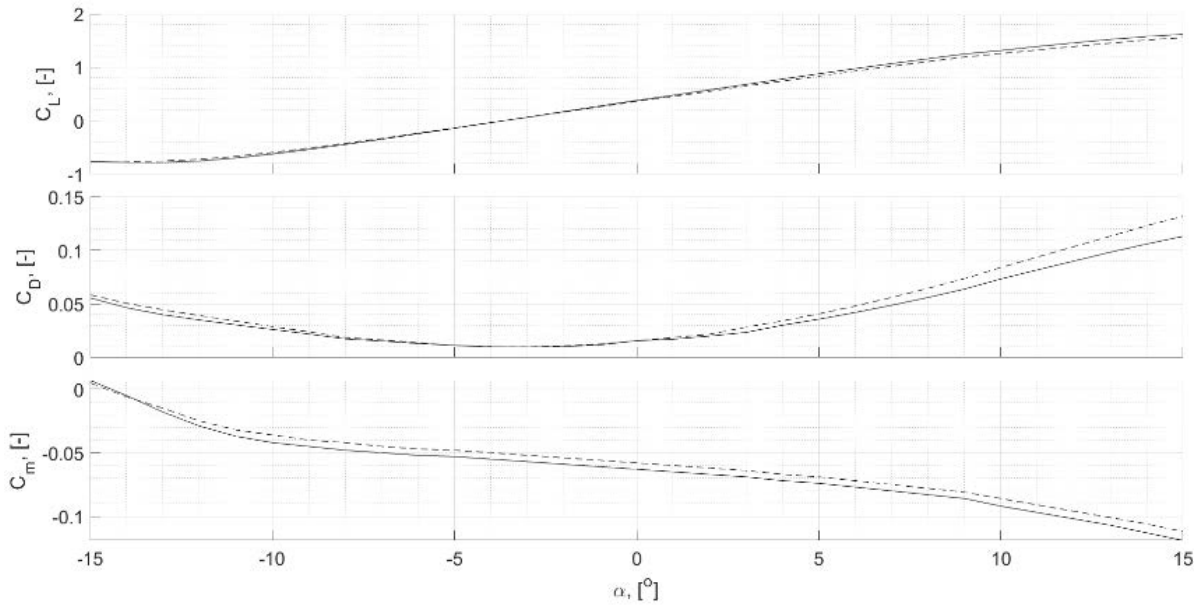


**Figure 5. $C_L$, $C_D$ and $C_m$ coefficients of forward (—) and aft (- - -) wings**

## 3.3 Bristol radar

The Primary Surveillance Radar (PSR) of the type of the Airport Surveillance Radar (ASR-11) [18] at the Bristol aerodrome was modelled to determine the radar coverage for the flight under investigation. Its parameters are provided in Table 2.

**Table 2. Bristol aerodrome radar**

| | | | |
|---|---|---|---|
| **Type** | Monostatic | **Beamwidth, deg** | 5 |
| **Mode** | Search track | **Frequency, GHz** | 3 |
| **Antenna beam pattern** | Cosecant squared | **Vertical half angle, deg** | 25 |
| **Sidelobe** | Parabolic | **Horizontal half angle, deg** | 0.75 |
| **Sensor type** | Rectangular | **Spin rate, rpm** | 15 |
| | | **Max range, km** | 150 |
| | | **Pulse repetition frequency, kHz** | 1 |
| | | **Pulse width, µs** | 1 |

The estimated maximum line of sight slant range $R$ on the spherical Earth limited by the horizon was 77 NM at the tower height $h_T = 91.9\ ft$ and aircraft altitude $h_R = 3000\ ft$. This figure is more conservative than the maximum ASR-11 detection range at the transmitter's standard capability (typically 25 kW RF peak power on an S-band carrier).

### 3.4 GPS coverage

The availability of GPS coverage and navigation accuracy was analysed over the flight path on a grid area of interest bounded by 51°15' - 51°45' N and 2°30' - 3°15' W and with a grid resolution of 1'30". The coordinates of the Avonmouth helipad and Cardiff heliport are provided in Table 3.

**Table 3. Coordinates of Avonmouth, England and Cardiff, Wales helipads**

| | **Latitude** | **Longitude** |
|---|---|---|
| **Avonmouth, England helipad** | 51° 30' 21" N | 2° 42' 58" W |
| **Cardiff, Wales heliport** | 51° 28' 03" N | 3° 08' 15" W |

## 4.0 RESULTS

### 4.1 Static stability for horizontal (cruise) flight

Two options of eVTOL configurations were chosen to investigate the effect of both elevon deflection and frame rotation on the static stability, i.e. $C_{m_\alpha}$ vs $X_{CG}$.

Figure 6 presents three static stability datasets for different control surface configurations, i.e. with zero elevon deflection and elevons deflected by ± 8°. CG values for neutral static stability correspond to 0.65 m for $\delta_{elevon} = +8°$ (positive elevon deflection creates negative pitching moment) and 0.68 m for $\delta_{elevon} = -8°$ (negative elevon deflection creates positive pitching moment).

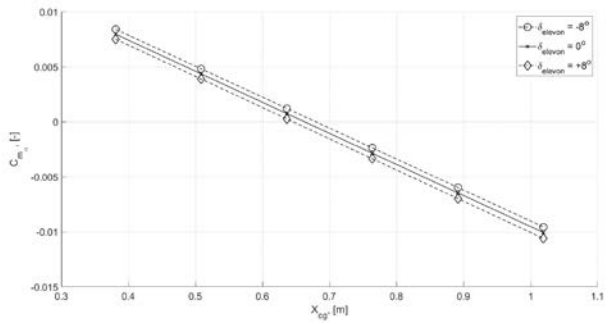

**Figure 6. $C_{m_\alpha}$ vs $X_{CG}$ graph showing statically stable airframe at 55 m/s with 0° frame setting angle**

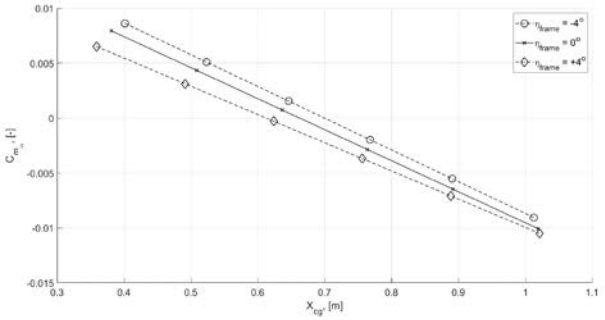

**Figure 7. $C_{m_\alpha}$ vs $X_{CG}$ graph showing statically stable airframe at 55 m/s with 0° elevon setting angle**

Figure 7 shows three static stability datasets for different frame configurations, i.e. with zero (cruise) rotation of the frame and with ± 4° rotation of the frame. CG values for neutral static stability correspond to 0.61 m for $\eta_{frame} = +4°$ and 0.70 m for $\eta_{frame} = -4°$.

In both options, we see a statically stable range of CGs forward of 0.67 m for zero elevon and zero frame configuration. It is important to notice that in both figures the first points on the left represent the original mass distribution for the eVTOL, clearly showing a statically unstable airframe.

Keeping in mind the fact that CG needs to be at least 0.67 m in front of the reference point, the eVTOL flight was then simulated and the time histories of its position and attitude were transferred to the STK Aviator for the analysis of radar and GPS coverage.

## 4.2 Radar coverage

The target probability of detection is the main outcome of the modelling and simulation of PSR and is shown in Figure 8. As the eVTOL aircraft is over the ground toward Bath and turns back toward Cardiff at about 11:02, the probability of detection is above 99.5%. When the flight is over the Severn Estuary, i.e. area of water at about 11:07, the probability of detection begins falling. The main reason for this is the inability of the tool to capture the free space path losses such as scatter, reflection, diffraction, atmospheric absorption, and isotropic spreading over irregular terrain and seawater. The detection rate, however, is at least 96% throughout the journey and follows the range.

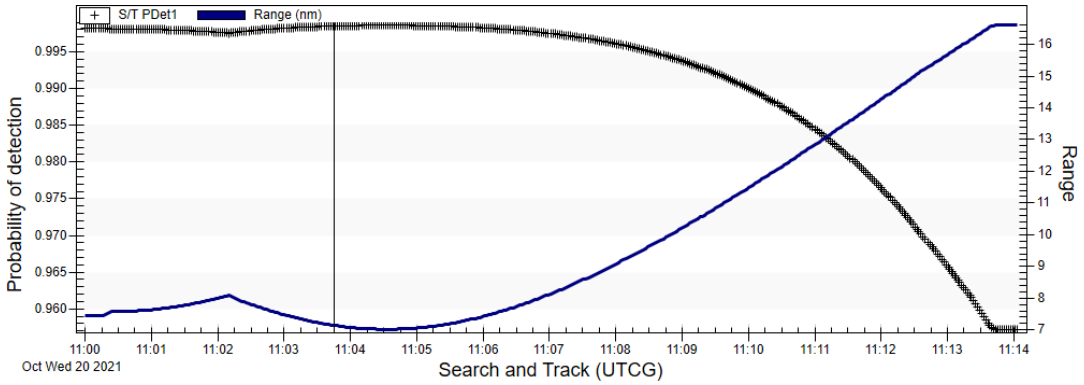


**Figure 8. Probability of detection and target range from radar**

## 4.3 GPS coverage

Figure 9 shows the GPS-provided accuracy for the route between Avonmouth and Cardiff. The contour plot changes with time, hence enabling the user of the programme to determine the best time for the flight in terms of the GPS position accuracy.

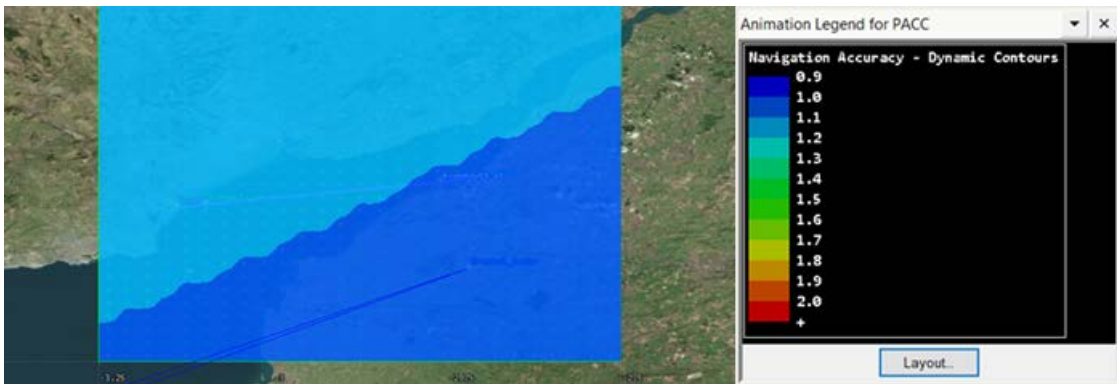


**Figure 9. Contours of GPS accuracy in meters**

The position accuracy (PACC) provided by GPS depends on the number of satellites in sight and, hence, changes over time. The above figure demonstrates the change of 0.9 m accuracy (dark blue) to 1.2 m accuracy (light blue).

# 5.0 DISCUSSION

The developed framework combines two software packages, very different in terms of their purposes. The MATLAB/Simulink package provides an easy-to-use maths-based environment to develop a flight dynamics

model of an eVTOL prototype aircraft. However, the visualisation of the flight of an eVTOL would be rather a challenging task to perform using the MATLAB/Simulink environment. Moreover, adding capabilities such as radar tracking and/or GPS coverage for the flight mission would require extensive effort. Hence, the STK software package supports the visualisation and additional features within the framework. The only drawback of the current framework is its inability to tightly couple both software packages into an automated loop, where the flight dynamics model would provide the required states of aircraft to the STK package.

Another advantage of such a framework is the ultimate user's control over the flight dynamics model. This means that any type of aircraft could be modelled, whether it be eVTOL, highly deformable wing large transport aircraft or a simple classic tube-and-wing aircraft configuration. This is extremely important when thinking about the transient effects, such as wing deformations under turbulent flight conditions or eVTOL reconfiguration during the transition phase. These effects cannot be modelled by simply using look-up-tables of aerodynamic coefficients. Although such an approach is presented in this paper, the reader must consider the fact that only eVTOL in cruise configuration was investigated. Moreover, the purpose of this paper is to present the framework and its capabilities, and an approach chosen to develop it, rather than an aerodynamic model. Hence, the paper clearly shows the capability of the framework to predict the GPS and radar coverage for the flight mission simulated using the flight dynamics model. Both cases clearly evidence the capability of PSR and GPS surveillance of the eVTOL aircraft in the given example. Although radar's capability to detect depends on the radar cross-section of a target and, hence, could reduce the probability to detect a small aircraft, the navigation accuracy provided by the GPS is an order of magnitude greater than the dimensions of the vehicle under investigation.

Moreover, as seen in Figure 6 the most left data point, the framework also showed that the initial mass distribution of the eVTOL led to the statically unstable airframe. Although such an engineering approach may be argued that there are control systems available to adjust the controls in a way that the pilot would perceive the aircraft as controllable (examples of inherent static instability of jet fighters), it must be understood that eVTOLs will be remotely piloted or unpiloted, hence carrying payload (cargo and/or passengers), who are not familiar with aircraft controls. Hence, it is vital to have a statically stable airframe. The static stability of an airframe is one of the aspects that the user can investigate using the proposed framework for developing digital twin prototypes.

## 6.0 CONCLUSIONS AND FURTHER WORK

The paper presented the framework for developing digital twin prototypes. The framework consists of two software packages, i.e. MATLAB/Simulink for flight dynamics modelling and simulation, STK Aviator for visualisation of the flight mission and additional features such as GPS coverage and radar tracking. A case study using the proposed framework was presented. It included the development of the flight dynamics model of an eVTOL aircraft and simulating its flight mission using the MATLAB/Simulink package. Then aircraft's position and attitude data were transferred to STK Aviator for route visualisation and analysis of GPS coverage and radar tracking. Estimates of the GPS signal accuracy were shown to be 0.9-1.2 m for the flight route, while the radar tracking model showed the probability of detection of more than 96% throughout the route. Moreover, the flight dynamics model was used to analyse the static stability of an aircraft and the analysis showed that the original centre of gravity location should be moved forward by around 0.3 m to ensure the airframe's static stability.

The authors plan further improvements to the framework in terms of coupling the MATLAB/Simulink and STK Aviator packages to enable automatic data exchange. The third element of the loop – a pilot – will be introduced by integrating the flight dynamics model with the flight simulator at the University of Nottingham, hence closing the feedback loop of the flight mission decision-making based on the visuals provided by the STK Aviator tool.

## ACKNOWLEDGEMENTS

The authors would like to thank Arnaud Didey, the founder of Neoptera Aero Ltd, for sharing the technical details of the eVTOL aircraft.

## REFERENCES

[1] M. Shafto *et al.*, 'Draft modeling, simulation, information technology & processing roadmap', NASA, Washington, DC, Nov. 2010.

[2] M. Grieves and J. Vickers, 'Digital twin: mitigating unpredictable, undesirable emergent behavior in complex systems', in *Transdisciplinary Perspectives on Complex Systems*, F.-J. Kahlen, S. Flumerfelt, and A. Alves, Eds. Cham, Switzerland: Springer International Publishing, 2017, pp. 85–113.

[3] Michael Bruno, 'Digital delay', *Aviation week & space technology*, vol. 184, no. 12, p. 11, Jun. 13, 2022.

[4] GAO, 'Transforming aviation: stakeholders identified issues to address for "Advanced Air Mobility"', U.S. Government Accountability Office, Washington, DC, GAO-22-105020, May 2022.

[5] D. G. Mitchell, D. H. Klyde, M. W. Shubert, D. Sizoo, and R. Schaller, 'Testing for certification of urban air mobility vehicles', presented at the AIAA SciTech 2022 Forum, San Diego, CA & Virtual, Jan. 2022. doi: 10.2514/6.2022-0889.

[6] M. Jones, A. Berg, D. H. Klyde, J. Miller, R. Heffley, and A. Arencibia, 'Using pilot models to support urban air mobility design, analysis and certification', presented at the AIAA Aviation 2022 Forum, Chicago, IL & Virtual, Jun. 2022. doi: 10.2514/6.2022-3942.

[7] Anonymous, 'Handling qualities requirements for military rotorcraft', United States Army Aviation and Missile Command, Redstone Arsenal, AL, Aeronautical design standard: Performance specification ADS-33E-PRF, Mar. 2000.

[8] D. J. Moorhouse and R. J. Woodcock, 'Background information and user guide for MIL-F-8785C, military specification - Flying qualities of piloted airplanes', USAF Wright Aeronautical Laboratories, Wright-Patterson AFB, OH, AFWAL-TR-81-3109, Sep. 1981.

[9] AGARD, 'V/STOL handling qualities criteria. 1 - Criteria and discussion', Advisory Group for Aerospace Research and Development, Neuilly-sur-Seine, France, AGARD-R-577-70, Dec. 1970.

[10] C. R. Chalk, D. L. Key, J. Jr. Kroll, R. Wasserman, and R. C. Radford, 'Background information and user guide for MIL-F-83300, military specification - Flying qualities of piloted V/STOL aircraft', Air Force Flight Dynamics Laboratory, Wright-Patterson AFB, OH, AFFDL-TR-70-88, Mar. 1971.

[11] J. A. Franklin, 'V/STOL dynamics, control, and flying qualities', NASA Ames Research Center, Moffett Field, CA, NASA/TP-2000-209591, Oct. 2000.

[12] EASA, 'Special Condition for small-category VTOL aircraft', European Aviation Safety Agency, Cologne, Germany, SC-VTOL-01, Jul. 2019.

[13] V. Portapas, Y. Zaidi, J. Bakunowicz, D. Paddeu, A. Valera-Medina, and A. Didey, 'Targeting global environmental challenges by the means of novel multimodal transport: Concept of operations', London, UK, Jul. 2021, pp. 101–106. doi: 10.1109/WorldS451998.2021.9514048.

[14] Martin Hepperle, 'JavaFoil user's guide', User guide, Dec. 2017.

[15] NIMA, 'World Geodetic System 1984', National Imagery and Mapping Agency, St. Louis, MO, TR8350.2, Jan. 2000.

[16] M. Kayton and W. R. Fried, Eds., *Avionics navigation systems*, 2nd ed. New York, NY: Wiley, 1997.

[17] H. W. Cole, *Understanding radar*, 2nd ed. Oxford, UK: Blackwell Scientific Publications, 1992.

[18] R. Weber and J. Schanne, 'Airport surveillance radar model 11 (ASR-11)', U.S. Department of Transportation Federal Aviation Administration, Atlantic City International Airport, NJ, FAA test and evaluation master plan (TEMP) DOT/FAA/CT-TN97/27, Feb. 1998.